

# A Classical Analogue of Entanglement for a Kicked Top

Bilal Khalid<sup>†</sup> and Sabre Kais<sup>\*,‡</sup>

<sup>†</sup>*Department of Physics and Astronomy, Purdue University, West Lafayette, IN-47907, USA*

<sup>‡</sup>*Department of Electrical and Computer Engineering, North Carolina State University, Raleigh, NC-27606, USA*

E-mail: skais@ncsu.edu

## Abstract

The kicked top is one of the most extensively studied paradigms of quantum chaos. The dynamics in this model are governed by a free precession of angular momentum interspersed with a periodic sequence of impulsive kicks. In previous studies, this system has been realized as a chain of spins-1/2 and an intricate connection has been observed between entanglement entropy of a single spin-1/2 and the classical dynamics. The initial conditions for which the classical dynamics are chaotic have been found to entail a greater entanglement entropy production than for ones that are classically regular. This connection appears surprising since both chaos and entanglement are understood to be exclusive to classical and quantum mechanics respectively.<sup>1</sup> In this paper, however, we have argued that from an alternative standpoint on classical physics, this connection becomes completely natural. In the mainstream approach to classical physics, an assumption that is accepted without question is the *principle of infinite precision*;<sup>2</sup> that physical quantities can be specified to an infinite number of digits. However, this assumption is hard to maintain on both ontological and epistemological grounds.

Dropping this assumption amounts to replacing infinitely precise points in phase space with phase space densities as more accurate representations of classical states. In this picture, many properties that have traditionally been held to be exclusively quantum appear in classical physics too. One such property is the *non-separability* of states, known as entanglement in the context of quantum mechanics. Looking at the kicked top from this paradigm of classical physics provides a completely fresh outlook to the chaos-entanglement discussion. A concrete correlation is observed between a classical notion of non-separability as quantified by mutual information and the quantum entanglement entropy. This finding opens up new avenues of understanding in quantum chaos and the more general problem of classical-quantum correspondence.

## 1 Introduction

Quantum chaos is the study of the quantum mechanical properties characteristic of systems that exhibit chaos classically. Traditionally, much attention has been devoted to the ascertainment of universal features in the spectral statistics of chaotic Hamiltonians.<sup>3</sup> However, more recent studies have also brought into the picture other quantum properties, a prominent one being quantum entanglement. Within this purview, an intricate link between classical chaos and quantum entanglement has been suggested. It has been observed that minimum uncertainty wave packets centered in regions of phase space that are classically chaotic entail more entanglement entropy production in the system than in regions that are classically regular.<sup>1,4-10</sup>

A system for which the chaos-entanglement relationship has been extensively studied is the kicked top model.<sup>1,4-7</sup> In this system, the evolution of the angular momentum  $\mathbf{J}$  (“the top”) is governed by two kinds of processes: (i) precession of  $\mathbf{J}$  around a fixed axis at a constant rate and (ii) a periodic sequence of kicks that bring about an instantaneous change in  $\mathbf{J}$ . The Hamiltonian for this system commutes with  $\mathbf{J}^2$ , so the quantum evolution is confined within a subspace characterized by an eigenvalue  $j(j+1)$  of  $\mathbf{J}^2$ . Moreover, the

model is chaotic in the classical limit  $j \rightarrow \infty$ . This model was introduced by Haake et al. to study how chaos arises as the system is made more and more classical.<sup>11</sup>

A particularly interesting realization of this model is in terms of a collection of spins-1/2 where  $\mathbf{J}$  becomes the collective angular momentum of the spins. We can then track the entanglement entropy of a single spin as a function of time and the initial state. By initializing the system in a spin-coherent state i.e. a minimum uncertainty angular momentum state, it has been observed that the entanglement entropy of a single spin has a strong correlation with the corresponding classical dynamics. For an initial state centered in a classically chaotic region of phase space, more entanglement entropy is produced than for one centered in a classically regular region.<sup>1,4-7</sup>

With the dramatic advancement in quantum simulation technologies over the last two decades, there has also been a lot of interest in experimental implementations of the kicked top Hamiltonian.<sup>1,4</sup> This was first achieved by Chaudhury et al. using the  $F = 3$  hyperfine ground state of  $^{133}\text{Cs}$ .<sup>4</sup> In their experiment, the total angular momentum in the Hamiltonian was taken to be the sum of the electron and nuclear spins of a single  $^{133}\text{Cs}$  atom. Consequently, the theoretically predicted correspondence between entanglement, as quantified by the linear entropy of the electron spin, and classical dynamics was corroborated. Later, similar conclusions were obtained by Neill et al. in their quantum simulation experiment of the same Hamiltonian using a three-qubit ring of planar transmons.<sup>1</sup> Commenting on their findings they added, “it is interesting to note that chaos and entanglement are each exclusive to their respective classical and quantum domains, and any connection is surprising.”

The connection is surprising because a purely quantum property is being related with a purely classical one, each one understood to have no counterpart on the other side. In this paper, however, we approach this connection not as a mere mathematical curiosity but as a clue hinting towards some profound insight into the classical-quantum relationship. We argue that the entanglement-chaos relation, and likewise many other relations between quantum and classical entities, appear surprising merely because of how we have come to formulate

classical and quantum mechanics; that in an alternative paradigm, such connections might seem perfectly natural.

It has been suggested previously that the exclusively quantum character which is ascribed to many properties of systems such as probabilities, entanglement etc. relies on a hidden assumption that is taken for granted in classical mechanics.<sup>2,12-16</sup> This is the assumption of infinite precision: that physical quantities can be specified to an infinite number of digits.<sup>2,12</sup> Under this assumption, classical mechanics becomes a fully deterministic and entanglement-less theory. However, this assumption has been challenged on both ontological (the nature of reality) and epistemological (the nature of knowledge) grounds. For instance, it has been argued that a finite volume of space can only hold a finite amount of information, whereas a real number contains an infinite number of bits.<sup>2,12</sup> Moreover, quantum mechanics itself seems to render impossible the existence of an infinitely precise value for a physical quantity. Furthermore, even if a physical quantity could take on an infinitely precise value, it would still be impossible to ascertain it to an infinite precision in a measurement.<sup>17</sup>

Classical physics without the assumption of infinite precision provides a completely fresh outlook to the discussion. Once this assumption is dropped, many quantum-like features become clearly noticeable even in classical physics that were otherwise hidden from view. For instance, a probabilistic view of physics instead of a deterministic one becomes natural.<sup>2,12</sup> In this paper, we are interested in investigating the prospects of yet another remarkable quantum property, namely entanglement, in this classical worldview.

The implausibility of infinite precision amounts to saying that the more accurate way to think about the states of classical systems is in terms of phase space densities instead of infinitely precise points in phase space. What then could be an analogue of entanglement in this picture? To make the analogy most transparent, it would be helpful to consider the meaning of entanglement in the Wigner function formalism of quantum mechanics as it provides a visualization of quantum states in phase space. In this formulation, the state of a quantum system is represented by a real-valued function in phase space  $W(\mathbf{q}, \mathbf{p})$ , called

the Wigner function. This function in many ways acts like the classical phase space density  $\rho(\mathbf{q}, \mathbf{p})$ . However, an important difference is that  $W(\mathbf{q}, \mathbf{p})$  is not really a distribution as it can take negative values unlike  $\rho(\mathbf{q}, \mathbf{p})$ .<sup>18,19</sup>

In the Wigner function formalism, two systems are entangled iff their collective Wigner function is non-separable i.e. if  $W(\mathbf{q}_1, \mathbf{q}_2, \mathbf{p}_1, \mathbf{p}_2)$  is the Wigner function of the total system and  $W_1(\mathbf{q}_1, \mathbf{p}_1) = \int W(\mathbf{q}_1, \mathbf{q}_2, \mathbf{p}_1, \mathbf{p}_2) d\mathbf{q}_2 d\mathbf{p}_2$  and  $W_2(\mathbf{q}_2, \mathbf{p}_2) = \int W(\mathbf{q}_1, \mathbf{q}_2, \mathbf{p}_1, \mathbf{p}_2) d\mathbf{q}_1 d\mathbf{p}_1$  are the Wigner functions of systems 1 and 2 respectively, then  $W(\mathbf{q}_1, \mathbf{q}_2, \mathbf{p}_1, \mathbf{p}_2) \neq W_1(\mathbf{q}_1, \mathbf{p}_1) \times W_2(\mathbf{q}_2, \mathbf{p}_2)$ . A straightforward classical analogue can then be constructed in terms of the separability of phase space density  $\rho$  which is the classical counterpart of Wigner function  $W$ . The classical state would be considered separable iff  $\rho(\mathbf{q}_1, \mathbf{q}_2, \mathbf{p}_1, \mathbf{p}_2) = \rho_1(\mathbf{q}_1, \mathbf{p}_1) \times \rho_2(\mathbf{q}_2, \mathbf{p}_2)$  and non-separable otherwise, where  $\rho_1(\mathbf{q}_1, \mathbf{p}_1) = \int \rho(\mathbf{q}_1, \mathbf{q}_2, \mathbf{p}_1, \mathbf{p}_2) d\mathbf{q}_2 d\mathbf{p}_2$  and  $\rho_2(\mathbf{q}_2, \mathbf{p}_2) = \int \rho(\mathbf{q}_1, \mathbf{q}_2, \mathbf{p}_1, \mathbf{p}_2) d\mathbf{q}_1 d\mathbf{p}_1$ .<sup>16</sup> The degree of non-separability can be quantified using mutual information which for two random variables  $X_1$  and  $X_2$  is defined as  $I_{12} = \int_{X_1} \int_{X_2} \rho(X_1, X_2) \log \left[ \rho(X_1, X_2) / (\rho_1(X_1)\rho_2(X_2)) \right] dX_1 dX_2$ .  $I_{12} \geq 0$  and  $I_{12} = 0$  iff  $\rho(X_1, X_2) = \rho_1(X_1)\rho_2(X_2)$ .

In this paper, we have conducted a test study of classical non-separability for the example of the kicked top. We have bi-partitioned the system and computed the mutual information between the variables lying across the partition. We observe remarkable similarity between mutual information on the classical side and entanglement as quantified by von-Neumann entanglement entropy on the quantum side.

These results are significant not just for the entanglement-chaos connection but also in the more general context of the classical-quantum relationship. In this picture, the relationship between chaos and entanglement can be reformulated essentially as a relationship between classical chaos and classical mutual information, of which quantum entanglement then becomes a reflection. More generally, this outlines a pathway to achieve a greater compatibility between quantum and classical physics. It is a step forward towards understanding quantum foundations which in its essence is concerned with delineating the precise

relationship between quantum and classical mechanics.<sup>20</sup>

The paper is organized as follows. Sec. 2 introduces the kicked top Hamiltonian and describes its classical dynamics. Sec. 3 then relates the correspondence between entanglement entropy and classical phase space for the kicked top. Moreover, we also plot a precise measure on the classical side, namely classical fluctuations  $(\Delta J)^2/J^2$ , for comparison with quantum entanglement entropy. Moving on, we plot classical mutual information as a function of the initial orientations and compare it with entanglement entropy in Sec. 4. Finally, we provide a summary of the results and an outlook for the future in Sec. 5.

## 2 Classical Dynamics

Consider the angular momentum operator  $\hbar\mathbf{J} = \hbar(J_x, J_y, J_z)$  satisfying the commutation relations  $[J_i, J_j] = i\varepsilon_{ijk}J_k$ . The Hamiltonian for the kicked top is then expressed in terms of  $\mathbf{J}$  as,<sup>11</sup>

$$H(t) = \frac{\hbar p}{\tau} J_y + \frac{\hbar \kappa}{2j} J_z^2 \sum_{n=-\infty}^{+\infty} \delta(t - n\tau). \quad (1)$$

The first term describes the precession of the rotor around the  $y$ -axis at a rate  $p/\tau$ . The second term represents a periodic sequence of kicks separated by a period  $\tau$ . Intuitively, this term can be thought of as a sudden precession around the  $z$ -axis by an angle proportional to  $J_z/j$ , where  $j$  is the total angular momentum quantum number. Once we initialize our system in the subspace characterized by the eigenvalue  $j(j+1)$  of the operator  $\mathbf{J}^2$ , we stay within the same subspace for all times since  $[\mathbf{J}^2, H(t)] = 0$ .  $\kappa$  is a dimensionless constant which controls the strength of the kick. For this paper, we are going to choose  $p = \pi/2$  i.e. the top precesses around the  $y$ -axis by an angle  $\pi/2$  between successive kicks.

Working in the Heisenberg picture, we are interested in tracking the evolution of  $\mathbf{J}$  in time. The evolution of the operator  $J_i$  in  $n$  time steps can be represented as  $J_i^{(n)} = (U^\dagger)^n J_i U^n$ ,

where  $U$  is the unitary evolution corresponding to the interval  $\tau$  between successive kicks,<sup>11</sup>

$$U = e^{-i(\kappa/2j)J_z^2} e^{-i(\pi/2)J_y}. \quad (2)$$

The evolution of  $\mathbf{J}$  can be represented in terms of the following non-linear operator recursion relations which determine how some  $\mathbf{J} = \mathbf{J}^{(i)}$  is updated to  $\mathbf{J}' = \mathbf{J}^{(i+1)}$  after each time step,<sup>11</sup>

$$\begin{aligned} J'_x &= \frac{1}{2}(J_z + iJ_y) e^{-i\frac{\kappa}{j}(J_x - \frac{1}{2})} + \text{h.c.} \\ J'_y &= \frac{1}{2i}(J_z + iJ_y) e^{-i\frac{\kappa}{j}(J_x - \frac{1}{2})} + \text{h.c.} \\ J'_z &= -J_x. \end{aligned} \quad (3)$$

Defining the rescaled angular momentum as  $\mathbf{X} = \mathbf{J}/j$  and taking the classical limit  $j \rightarrow \infty$ , we can track the evolution of the now real-valued  $\mathbf{X} = (X, Y, Z)$  on the surface of a unit sphere using the following recursion relations obtained from (3),

$$\begin{aligned} X' &= \text{Re}\{(Z + iY) e^{-i\kappa X}\} \\ Y' &= \text{Im}\{(Z + iY) e^{-i\kappa X}\} \\ Z' &= -X. \end{aligned} \quad (4)$$

In Fig. 1, we have plotted some examples of the phase portraits in spherical coordinates (i.e.  $X = \sin\theta \cos\phi$ ,  $Y = \sin\theta \sin\phi$  and  $Z = \cos\theta$ ) that are produced by the recursion relations (4) for different values of the kicking strength  $\kappa$ . We can see that as we tune  $\kappa$  from low to high, the islands of regularity shrink and chaos starts to take over.

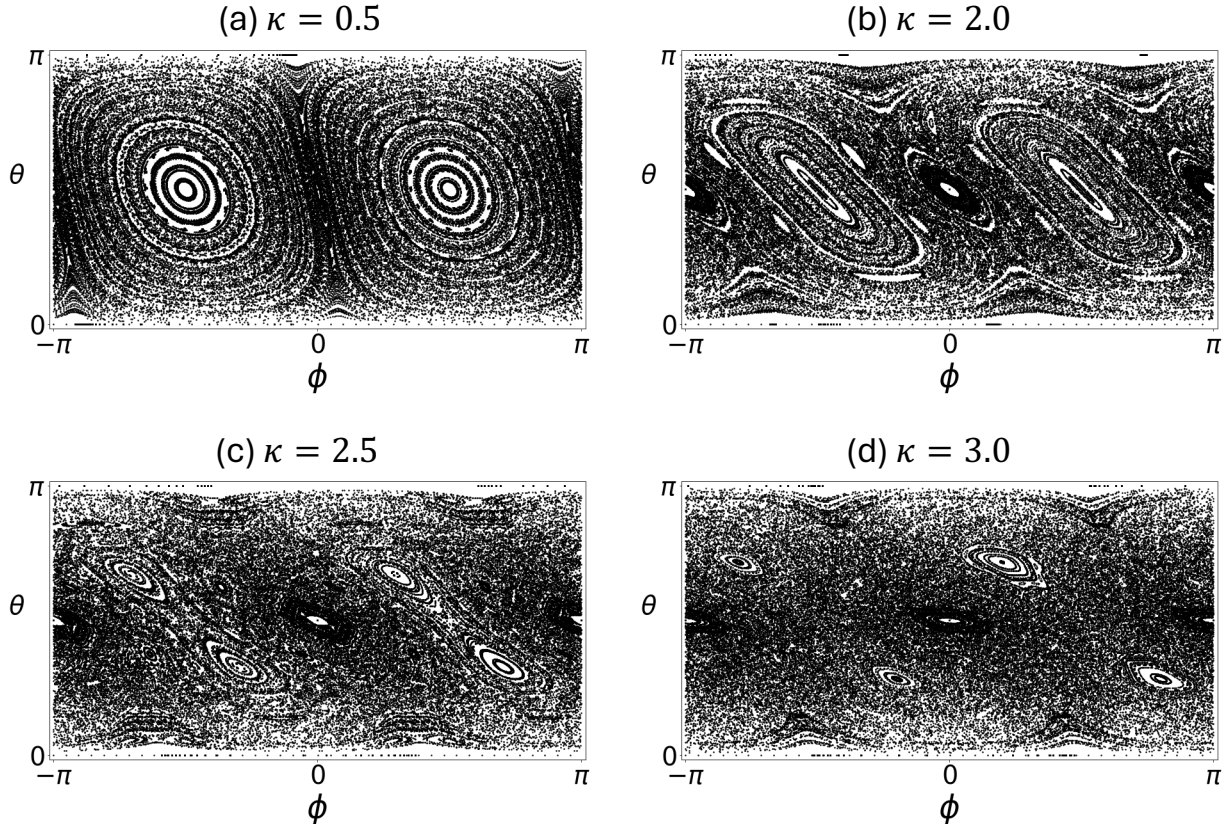


Figure 1: **Classical phase portraits for the kicked top.** The trajectories of rescaled angular momenta  $\mathbf{X} = \mathbf{J}/j$  are plotted in the classical limit  $j \rightarrow \infty$  with respect to the polar and azimuthal angles on a unit sphere. As the kick strength  $\kappa$  is increased, islands of regularity shrink and chaos takes over.

### 3 Entanglement Entropy and Classical Fluctuations

#### 3.1 Entanglement Entropy

Consider a collection of  $N$  spins-1/2 with the corresponding spin operators  $\mathbf{S}_i = (S_{ix}, S_{iy}, S_{iz})$  for the  $i$ th spin such that the dynamics of the total angular momentum  $\mathbf{J} = \sum_{i=1}^N \mathbf{S}_i$  is governed by the Hamiltonian (1). In terms of the spin operators  $\mathbf{S}_i$ , the Hamiltonian can be re-written as

$$H(t) = \frac{\hbar\pi}{2\tau} \sum_{i=1}^N S_{iy} + \frac{\hbar\kappa}{2j} \left( \sum_{i=1}^N S_{iz}^2 + \sum_{i \neq j} S_{iz} S_{jz} \right) \sum_{n=-\infty}^{+\infty} \delta(t - n\tau). \quad (5)$$

Before every kick, each spin independently precesses around the y-axis by an angle  $\pi/2$ . Noting that  $(\sum_{i=1}^N S_{iz}^2 + \sum_{i \neq j} S_{iz} S_{jz}) = J_z (\sum_{i=1}^N S_{iz})$ , the kick can be understood as causing a sudden precession of each spin around the z-axis by an angle proportional to  $J_z/j$ , a collective property of the spins.

We are interested in tracking the dynamics of the von-Neumann entanglement entropy of a single spin in this system. Suppose, we initialize our system in the state

$$|\psi(t=0)\rangle = \bigotimes_{i=1}^N |\theta_0, \phi_0\rangle_i, \quad (6)$$

where  $|\theta_0, \phi_0\rangle = \cos(\theta_0/2) |\uparrow\rangle + e^{-i\phi_0} \sin(\theta_0/2) |\downarrow\rangle$ . The state  $|\theta_0, \phi_0\rangle$  is geometrically represented as the point  $(\theta_0, \phi_0)$  on the Bloch sphere. We can evolve this state in time as  $|\psi(t=n\tau)\rangle = U^n |\psi(t=0)\rangle$ , where  $U$  is given in (2). The entanglement entropy of a spin at each time step can then be found using  $S(n) = -\text{Tr} \{\rho_1(n) \ln \rho_1(n)\}$  where  $\rho_1(n) = \text{Tr}_{i \neq 1} \{|\psi(t=n\tau)\rangle \langle \psi(t=n\tau)|\}$ . The choice of spin for calculating  $S$  is arbitrary since both the state and the Hamiltonian are symmetric with respect to all the spins.

In Fig. 2, we have plotted some example scenarios for the evolution of  $S$  in units of  $\ln 2$  which is the maximum possible value of  $S$ . Fig. 2(a) and (b) correspond to  $\kappa = 0.5$  when most of the phase space is regular, whereas for (c) and (d) we have  $\kappa = 2.5$  when chaos is dominant (see Fig. 1.) For the regular case in (a) and (b), we see that  $S$  reaches a peak and then periodically undergoes a series of collapses and revivals. As  $N$  increases, the time that  $S$  spends at its peak becomes greater and in the limit  $N \rightarrow \infty$ , we would expect  $S$  to stay at its peak for all times. For the chaotic case in (c) and (d), we find that  $S$  reaches its peak and then undergoes fluctuations around the peak that appear to be a bit more random. The fluctuations decrease in size as  $N$  becomes larger and in the limit  $N \rightarrow \infty$ , we expect the fluctuations to wither away.<sup>1,5</sup>

To obtain an estimate for the equilibrium value  $S_{\text{eq}}$  in the limit  $N \rightarrow \infty$ , we can extract the peak of  $S$  by performing an average over carefully chosen time steps for a finite  $N$ .<sup>1,5</sup> In

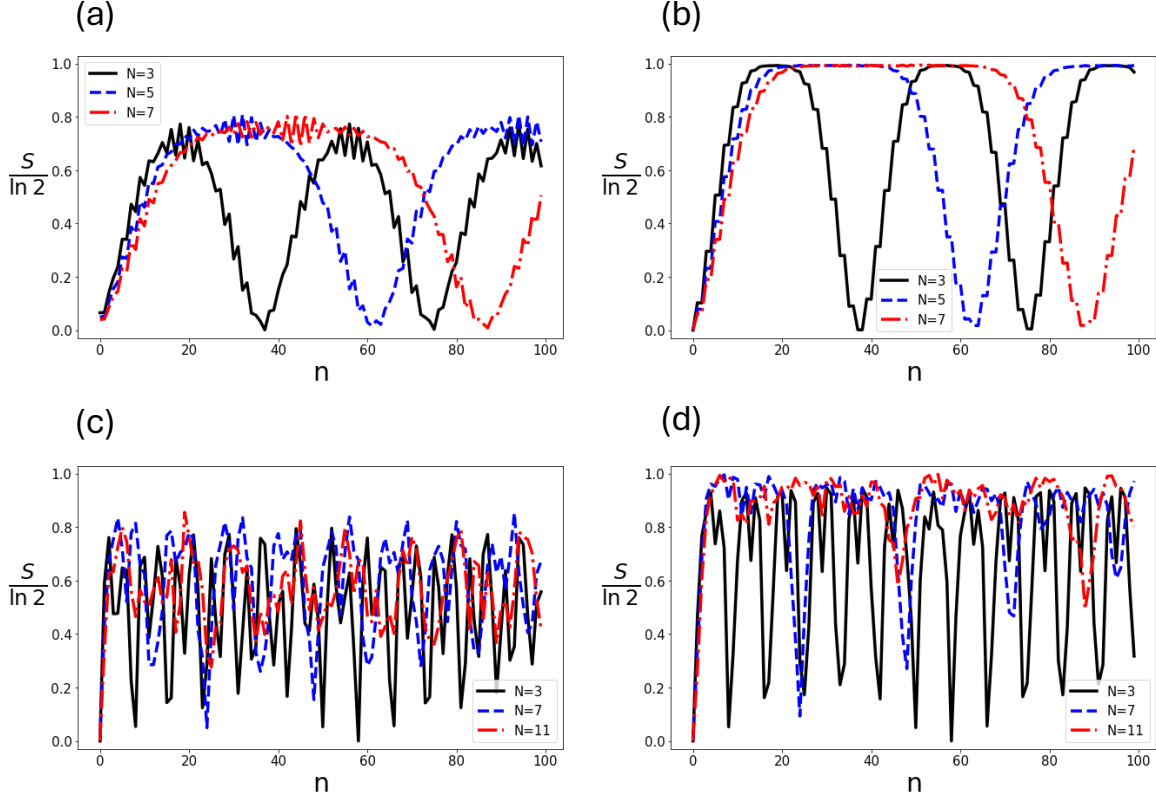


Figure 2: **Time evolution of entanglement entropy.** Entanglement entropy of a single spin  $S = -\text{Tr} \{ \rho_1 \ln \rho_1 \}$  in units of  $\ln 2$  as a function of the number of time steps  $n$ . (a) and (b) show the results for the regular regime  $\kappa = 0.5$  where we chose (a)  $\theta_0 = 3\pi/4$ ,  $\phi_0 = 3\pi/4$  and (b)  $\theta_0 = \pi/2$ ,  $\phi_0 = 0.1$ . (c) and (d) show the results for the chaotic regime  $\kappa = 2.5$  where the initial conditions were (c)  $\theta_0 = 3\pi/4$ ,  $\phi_0 = 3\pi/4$  and (d)  $\theta_0 = \pi/3$ ,  $\phi_0 = 3\pi/4$ . For both cases, we expect  $S$  to attain an equilibrium value in the limit  $N \rightarrow \infty$ .

Fig. 3(a) and (b), we have plotted our estimates of  $S_{\text{eq}}$  in units of  $\ln 2$  as a function of the initial conditions  $(\theta_0, \phi_0)$  for  $\kappa = 0.5$  and  $\kappa = 2.5$  respectively. Adjacent to the entanglement plots, we have also shown the corresponding classical phase portraits. We used 7 spins for both cases. For (a), we averaged  $S(n)$  over  $20 \leq n \leq 40$  whereas for (b), the average was computed over  $5 \leq n \leq 20$ . A remarkable similarity is observed between the entanglement plots and the classical phase portraits. Roughly speaking, as we go from a region with regular dynamics to a region where the dynamics is “more chaotic” in the classical phase space, we correspondingly move from a region of lower entanglement entropy to a region of higher entropy on the quantum side.<sup>1</sup> However, to make the comparison concrete, we need

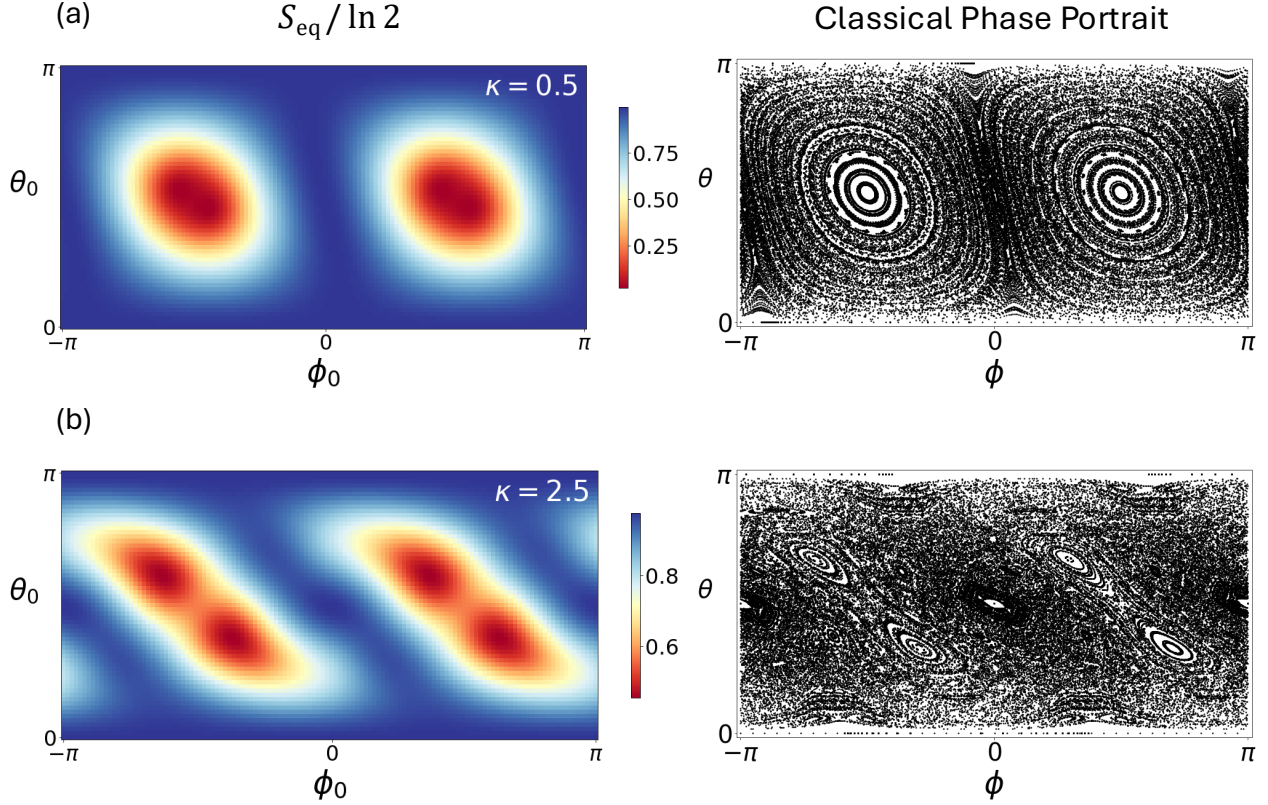


Figure 3: **Entanglement entropy and classical phase space.** Equilibrium values of entanglement entropy  $S_{\text{eq}}$  have been estimated as a function of the initial state  $(\theta_0, \phi_0)$ . For (a)  $\kappa = 0.5$ , the entanglement entropy was averaged over  $20 \leq n \leq 40$ . For (b)  $\kappa = 2.5$ , the average was computed over  $5 \leq n \leq 20$ . The size of the system for both cases was 7 spins. Beside each entanglement plot, the corresponding classical phase portrait has also been reproduced from Fig. 1. A remarkable similarity between the entanglement plots and the classical phase portraits is observed.

a classical measure on phase space for drawing a parallel with the entanglement entropy.

### 3.2 Classical Fluctuations

Let's write the most general density matrix for a single spin-1/2,

$$\rho = \begin{pmatrix} \frac{1}{2}(1 + r\cos\theta) & \frac{r}{2}e^{-i\phi}\sin\theta \\ \frac{r}{2}e^{-i\phi}\sin\theta & \frac{1}{2}(1 - r\cos\theta) \end{pmatrix}. \quad (7)$$

In this parameterization,  $\langle S_x \rangle = \frac{r}{2} \sin\theta \cos\phi$ ,  $\langle S_y \rangle = \frac{r}{2} \sin\theta \sin\phi$  and  $\langle S_z \rangle = \frac{r}{2} \cos\theta$  where  $0 \leq r \leq 1$ . The parameter  $r$  specifies the length of the Bloch vector representing the state. For  $r = 1$ , the vector lies on the surface of the Bloch sphere and the state is pure. For  $r < 1$ , the state is mixed. The eigenvalues of  $\rho$  are  $\frac{1}{2}(1 - r)$  and  $\frac{1}{2}(1 + r)$ . So, the von Neumann entropy for  $\rho$  can be calculated to be

$$S[\rho] = -\frac{1}{2}(1 - r)\ln\left[\frac{1}{2}(1 - r)\right] - \frac{1}{2}(1 + r)\ln\left[\frac{1}{2}(1 + r)\right]. \quad (8)$$

Thus,  $S = 0$  for  $r = 1$  and it increases monotonically as  $r$  is reduced until it reaches its maximum  $S = \ln 2$  for  $r = 0$  [see Fig. 4(a).]

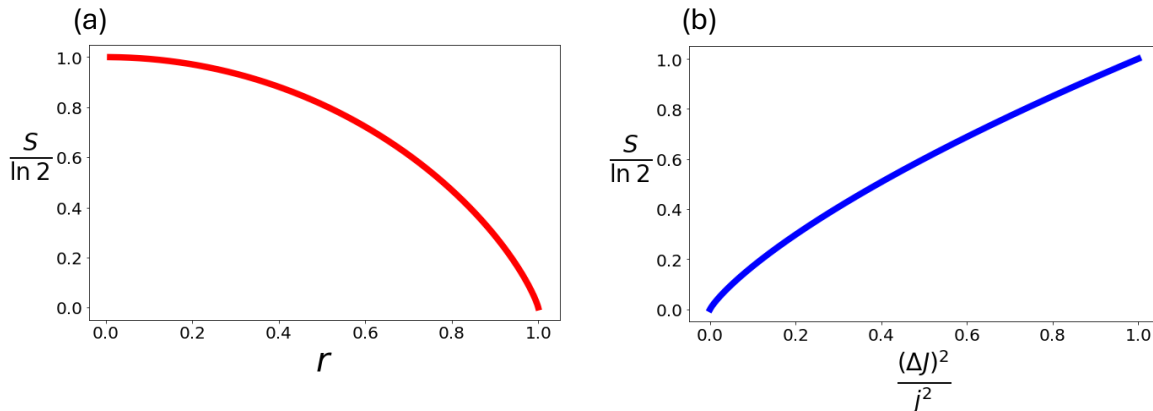


Figure 4: **Entanglement entropy and quantum fluctuations.** (a) Entanglement entropy  $S$  of a single spin-1/2 versus the length of its Bloch vector  $r$ . (b) Entanglement entropy  $S$  of a single spin-1/2 versus the relative variance  $(\Delta J)^2/j^2$  of the total angular momentum as  $j \rightarrow \infty$ .

For our case of  $N$  spins-1/2, we have  $\mathbf{J} = \sum_{i=1}^N \mathbf{S}_i$ . Since both the initial state and the Hamiltonian are symmetric with respect to all the spins, the state will retain this symmetry at all times. This implies that  $\langle \mathbf{S}_i \rangle = \langle \mathbf{J} \rangle / N$ . Using  $r^2/4 = \langle S_x \rangle^2 + \langle S_y \rangle^2 + \langle S_z \rangle^2$  and  $N = 2j$  we obtain

$$r^2 = \frac{j+1}{j} - \frac{(\Delta J)^2}{j^2}, \quad (9)$$

where  $(\Delta J)^2 = \langle \mathbf{J}^2 \rangle - \langle \mathbf{J} \rangle^2$ . In the limit  $j \rightarrow \infty$  (equivalent to  $N \rightarrow \infty$ ), this becomes

$$r^2 = 1 - \frac{(\Delta J)^2}{j^2}. \quad (10)$$

Thus, we have found a straightforward analytic relationship of the length of the Bloch vector for a single spin-1/2 and hence its entanglement entropy  $S$  [see (8)] with the relative variance  $(\Delta J)^2/j^2$  of the total angular momentum  $\mathbf{J}$  of the system. The larger the relative variance  $(\Delta J)^2/j^2$  of the total angular momentum in a given state, the greater will be the entanglement entropy  $S$  of a single spin-1/2, and vice versa. This relationship has been plotted in Fig. 4(b).

So far, we have seen that there is an exact relationship between quantum fluctuations  $(\Delta J)^2/j^2$  and the entanglement entropy of a single spin  $S$ . The question is if this relationship could be extended to classical fluctuations  $(\Delta J)^2/J^2$  (where  $j$  is replaced by  $J$  in the classical limit) as well? To explore this question, we first note that the initial state in (6) can also be written in the following form<sup>11</sup>

$$|\psi(t=0)\rangle = \bigotimes_{i=1}^N |\theta_0, \phi_0\rangle_i = \exp\{i\theta_0(J_x \sin \phi_0 - J_y \cos \phi_0)\} |j, j\rangle. \quad (11)$$

This is known as a spin coherent state. It is the minimum uncertainty angular momentum state pointing along a certain direction  $(\theta_0, \phi_0)$ .<sup>11</sup> In analogy with this state, we are now going to evolve a collection of trajectories using eqs. (4) initiating in a cloud of points centered at  $(\theta_0, \phi_0)$  and with the same angular spread  $\sin \theta_0 \Delta \theta \Delta \phi = 1/J$  as (11).<sup>11</sup> The initial points will be chosen uniformly from this cloud. Then we can compute  $(\Delta J)^2/J^2 = \langle \mathbf{X}^2 \rangle - \langle \mathbf{X} \rangle^2$  at any arbitrary time by averaging over all the trajectories.

In Fig. 5, we have compared the equilibrium values of  $(\Delta J)^2/J^2$  and the entanglement entropy  $S$ . The equilibrium values of fluctuations have been estimated by computing an average of  $(\Delta J)^2/J^2$  between  $400 \leq n \leq 500$  for both  $\kappa = 0.5$  and  $\kappa = 2.5$  (see supplementary information S-I for time variation of  $(\Delta J)^2/J^2$ .) For the initial states, we have

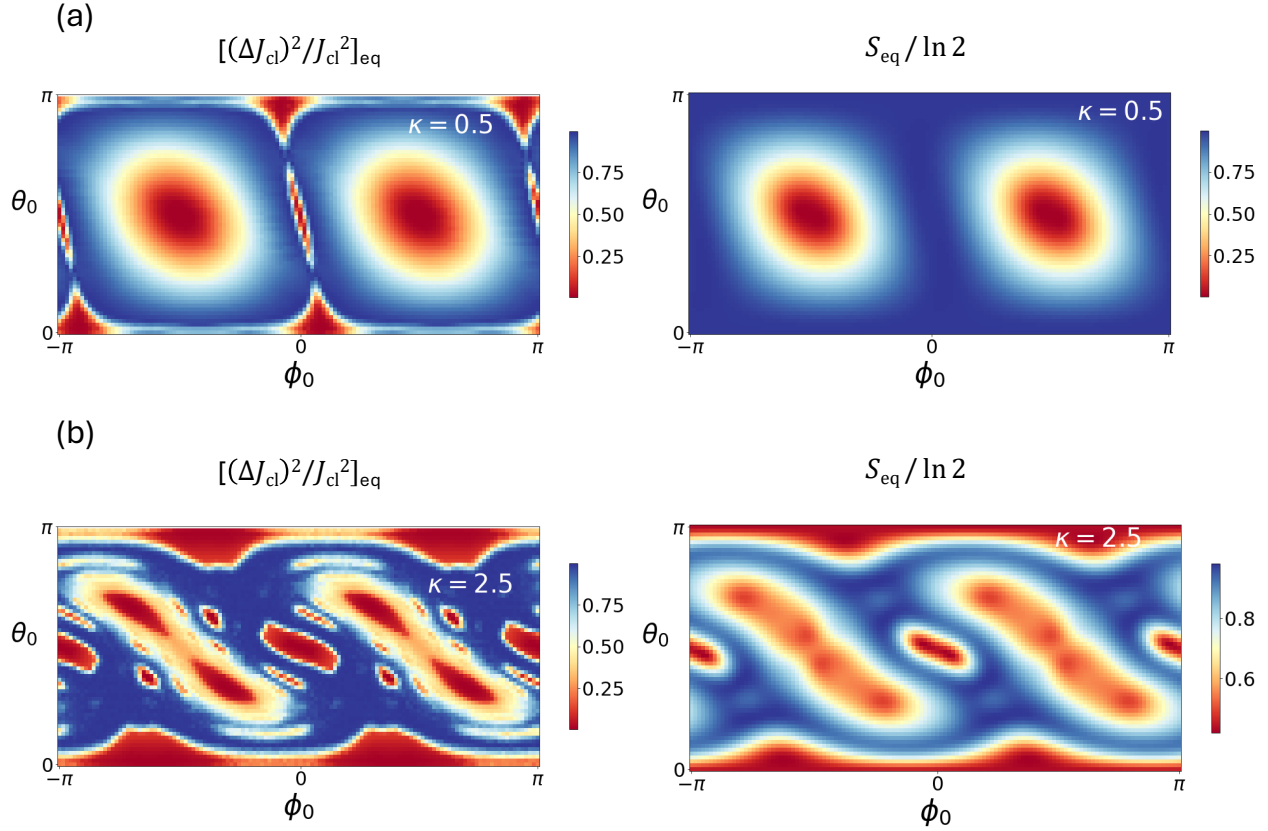


Figure 5: **Classical fluctuations and entanglement entropy.** A comparison of the equilibrium values of classical fluctuations  $(\Delta J)^2/J^2$  (on the left) and entanglement entropy  $S$  (on the right.) To estimate its equilibrium value, we have averaged  $(\Delta J)^2/J^2$  over  $400 \leq n \leq 500$ . For the initial states  $(\theta_0, \phi_0)$ , the angular spread was  $\sin \theta_0 \Delta \theta \Delta \phi = 1/J$  with  $J = 100$  and 100 trajectories were sampled. For  $S_{\text{eq}}$ , we have used eqs. (8) and (9) to convert quantum fluctuations to entanglement entropies. Entanglement entropies were averaged over  $60 \leq n \leq 100$  for  $\kappa = 0.5$ , and over  $20 \leq n \leq 40$  for  $\kappa = 2.5$ .

used  $\sin \theta_0 \Delta \theta \Delta \phi = 1/J$  with  $J = 100$ , and for each  $(\theta_0, \phi_0)$ , 100 trajectories were sampled. Moreover, to obtain better estimates for  $S_{\text{eq}}$  than in Fig. 3, we have converted quantum fluctuations  $(\Delta J)^2/j^2$  for  $j = 20$  ( $N = 40$ ) to  $S$  using eqs. (8) and (9), and then performed the corresponding averages. For  $\kappa = 0.5$ , the average is performed between  $60 \leq n \leq 100$ , whereas for  $\kappa = 2.5$ , the average is computed over  $20 \leq n \leq 40$  (see supplementary information S-II for the corresponding quantum fluctuations.) We can see from the figure that there is a wonderful resemblance between classical fluctuations  $(\Delta J)^2/J^2$  and quantum entanglement entropy  $S$ .

## 4 Classical Mutual Information

While we have made the duality more concrete, however, the two quantities being compared i.e. fluctuations  $(\Delta J)^2/J^2$  on one side and entanglement entropy  $S$  on the other, are conceptually very distinct. The former measures a collective effect of the entire system, whereas, the latter expresses the degree of correlation among the internal constituents of the system. Can we come up with a classical quantity that is more similar in philosophy to entanglement entropy?

While, traditionally, it has been understood that there is no classical analogue of entanglement, however, in the *Introduction*, we have motivated a classical analogue. This conception relies on replacing infinitely precise points with distributions in phase space to represent states of classical systems. One can then construct an analogue of entanglement in terms of the non-separability of a collective distribution  $\rho_{12}$  into  $\rho_1$  and  $\rho_2$ , in analogy with the non-separability of the Wigner function  $W_{12}$  for an entangled system (see Sec. 1.)

So, drawing a parallel with entanglement entropy, suppose we partition  $\mathbf{J}$  in (1) into  $\mathbf{J}_1$  and  $\mathbf{J}_2$  such that  $\mathbf{J} = \mathbf{J}_1 + \mathbf{J}_2$ . The Hamiltonian (1) can then be re-expressed in terms of  $\mathbf{J}_1$  and  $\mathbf{J}_2$  as

$$H(t) = \frac{\hbar\pi}{2\tau}(J_{1y} + J_{2y}) + \frac{\hbar\kappa}{2j}(J_{1z}^2 + J_{2z}^2 + 2J_{1z}J_{2z}) \sum_{n=-\infty}^{+\infty} \delta(t - n\tau). \quad (12)$$

$\mathbf{J}_1^2$  and  $\mathbf{J}_2^2$  are conserved quantities since  $[\mathbf{J}_{1,2}^2, H(t)] = 0$ . The unitary evolution operator over one cycle is  $U = U_{z2}U_{12}U_y$  where  $U_{z2} = e^{-i(\kappa/2j)J_{1z}^2}e^{-i(\kappa/2j)J_{2z}^2}$ ,  $U_{12} = e^{-i(\kappa/j)J_{1z}J_{2z}}$  and  $U_y = e^{-i(\pi/2)J_{1y}}e^{-i(\pi/2)J_{2y}}$ . We can compute  $\mathbf{J}'_1 = U^\dagger\mathbf{J}_1U$  to produce the following recursion relations for the update of angular momentum of subsystem 1 (see supplementary information

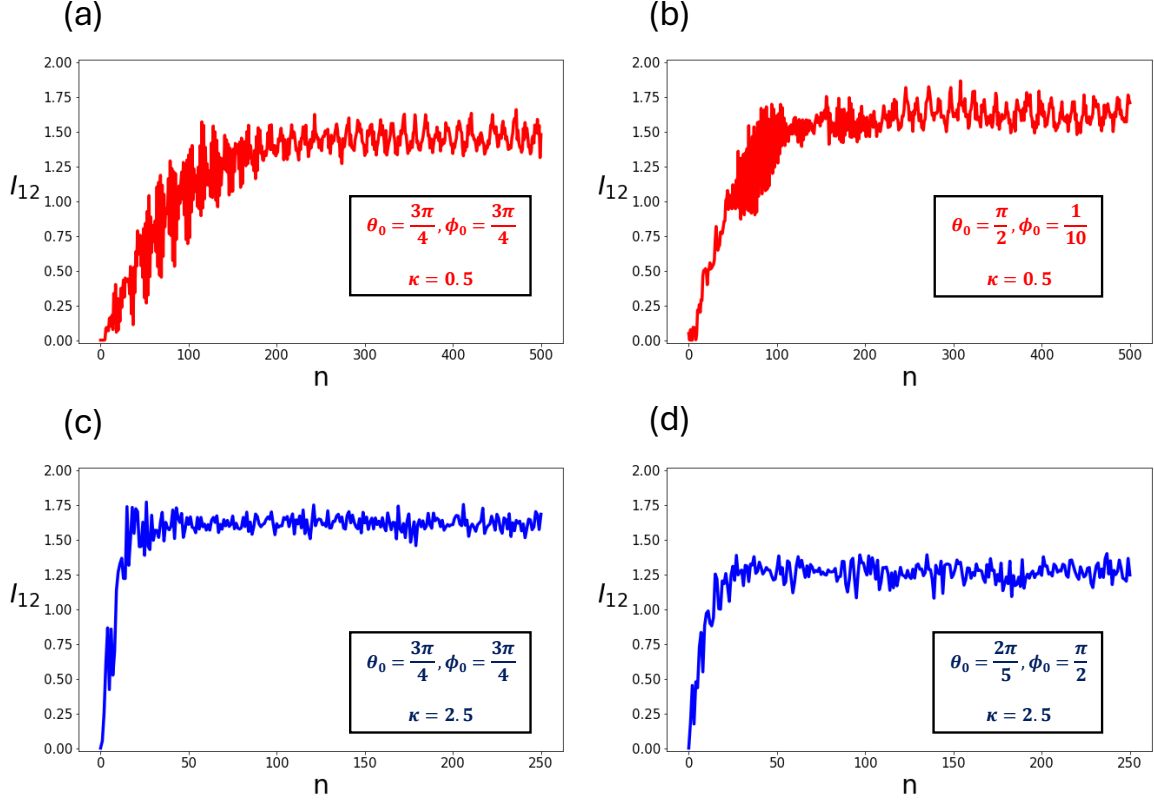


Figure 6: **Time evolution of mutual information.** Mutual information  $I_{12}$  between the variables  $X_1 = J_{1x}/J$  and  $X_2 = J_{2x}/J$  as a function of time  $n$ . For this calculation, we took  $J = 100$ ,  $X_1 = 1/(2J)$  and  $X_2 = J - X_1$ . The initial distribution was taken to be a uniform cloud of points of angular spread  $\sin \theta_0 \Delta \theta \Delta \phi = 1/4$  for 1 and a cloud of angular spread  $\sin \theta_0 \Delta \theta \Delta \phi = 1/J_2$  for 2, each centered at  $(\theta_0, \phi_0)$ . 300 trajectories were sampled for each case. We observe a faster approach to equilibrium for the chaotic case in (c) and (d) compared to the regular case (a) and (b), in analogy with entanglement entropy.

S-III.)

$$\begin{aligned}
 J'_{1x} &= \frac{1}{2}(J_{1z} + iJ_{1y}) e^{-i\frac{\kappa}{j}(J_{1x} + J_{2x} + \frac{1}{2})} + \text{h.c.} \\
 J'_{1x} &= \frac{1}{2i}(J_{1z} + iJ_{1y}) e^{-i\frac{\kappa}{j}(J_{1x} + J_{2x} + \frac{1}{2})} + \text{h.c.} \\
 J'_{1x} &= -J_{1x}.
 \end{aligned} \tag{13}$$

For  $\mathbf{J}'_2$ , we only need to interchange the indices 1 and 2 in the above equations. Finally,

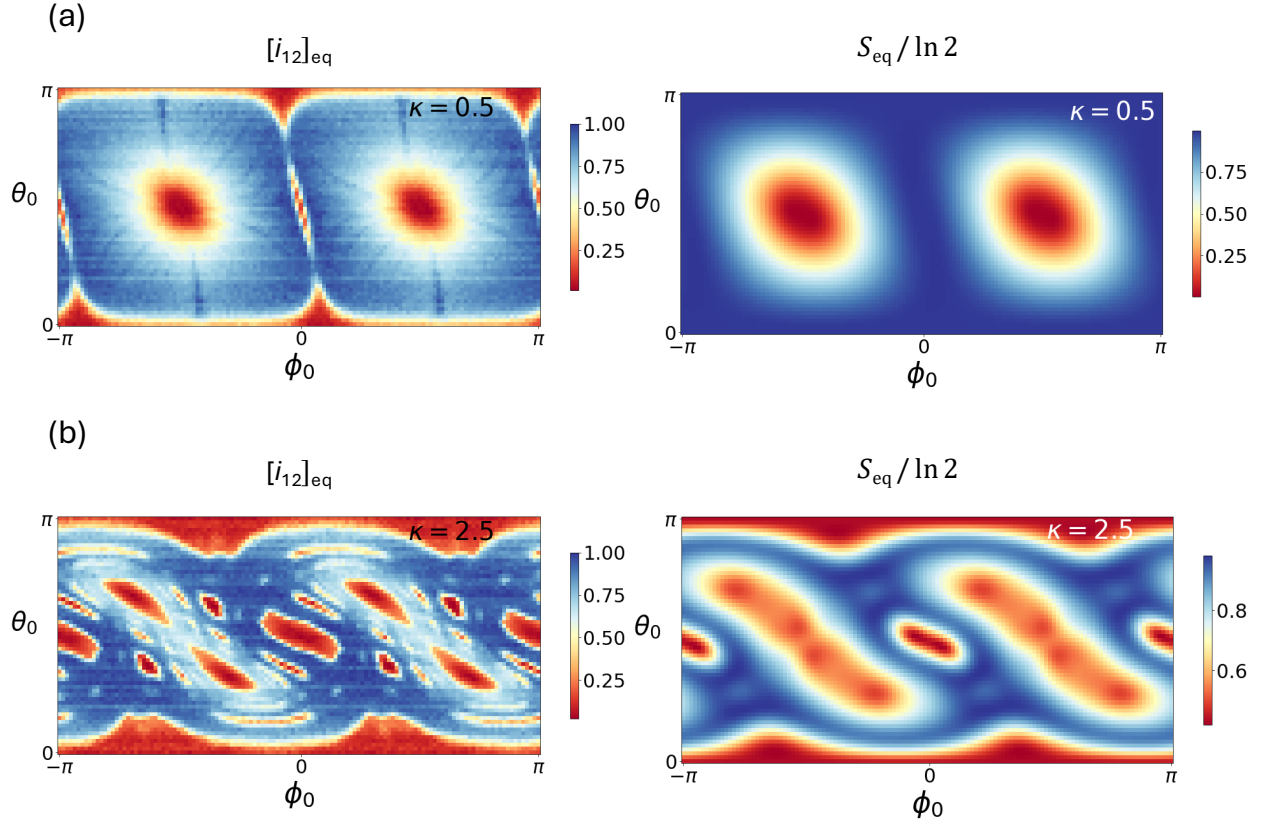


Figure 7: **Mutual information and entanglement entropy.** A comparison of rescaled equilibrium mutual information  $[i_{12}]_{\text{eq}}$  and entanglement entropy  $S_{\text{eq}}$ . For each  $(\theta_0, \phi_0)$ , the same parameters have been used to specify the initial distribution as for the calculation in Fig. 6. For (a), the average is performed over  $400 \leq n \leq 500$  and the normalization factor is  $[I_{12}]_{\text{eq}}^{\text{max}} = 1.77$ . For (b), the average is taken over  $100 \leq n \leq 150$  and the values have been scaled with  $[I_{12}]_{\text{eq}}^{\text{max}} = 1.59$ . The conceptual similarity of  $I_{12}$  and  $S$  makes the classical-quantum connection for this system much more transparent.

defining  $\mathbf{X}_{1,2} = \mathbf{J}_{1,2}/j$  and taking the classical limit  $j \rightarrow \infty$  we get

$$\begin{aligned}
 X'_1 &= \text{Re}\{(Z_1 + iY_1) e^{-i\kappa(X_1+X_2)}\} \\
 Y'_1 &= \text{Im}\{(Z_1 + iY_1) e^{-i\kappa(X_1+X_2)}\} \\
 Z'_1 &= -X_1.
 \end{aligned} \tag{14}$$

In analogy with (6), we can initialize our system in a distribution completely separable into sub-distributions for subsystems 1 and 2, each centered around  $(\theta_0, \phi_0)$ . Then, we can

sample some trajectories, evolve them using eqs. (14) and estimate mutual information with time. In Fig. 6, we have produced such a calculation. For this analysis, we chose  $J = 100$ . Taking  $\mathbf{X}_1$  to be an analogue of a single spin-1/2, we assigned  $X_1 = 1/(2J)$  for the initial distribution and  $X_2 = J - X_1$ , to ensure proper normalization of  $\mathbf{X} = \mathbf{X}_1 + \mathbf{X}_2$ . For the initial distribution of 1, we took a uniform cloud with an angular spread of  $\sin \theta_0 \Delta\theta \Delta\phi = 1/4^*$ , whereas for 2, we took  $\sin \theta_0 \Delta\theta \Delta\phi = 1/J_2$ . We then sampled 300 trajectories and estimated the mutual information  $I_{12}$  between the variables  $X_1 = J_{1x}/J$  and  $X_2 = J_{2x}/J$ . Fig. 6 shows the plots of  $I_{12}$  with time for four different scenarios. Like entanglement entropy in Fig. 2, we observe a much faster approach to equilibrium for the chaotic case in (c) and (d) compared to the regular case in (a) and (b).

Then, in Fig. 7, using the same strategy and parameters, we have estimated the equilibrium values of mutual information  $I_{12}$  as a function of the initial orientation  $(\theta_0, \phi_0)$ . For comparison, we have also reproduced the plots for entanglement entropy  $S$  from Fig. 5. For (a)  $\kappa = 0.5$ , the average for  $I_{12}$  is performed over  $400 \leq n \leq 500$  whereas for (b)  $\kappa = 2.5$ , the average is taken over  $100 \leq n \leq 150$ . Moreover, we have rescaled  $[I_{12}]_{\text{eq}}$  to have a maximum value of 1. This rescaling is done with  $[I_{12}]_{\text{eq}}^{\text{max}} = 1.77$  for  $\kappa = 0.5$  and  $[I_{12}]_{\text{eq}}^{\text{max}} = 1.59$  for  $\kappa = 2.5$ . Clearly, there is a remarkable similitude between mutual information  $I_{12}$  and entanglement entropy  $S$ . The conceptual similarity of the two quantities being compared underlies the true significance of this result. Each side of the duality is understood quite naturally in light of the other unlike previous comparisons.

## 5 Conclusion and Outlook

In this paper, we have re-framed a problem of quantum chaos in an alternative paradigm of classical physics. In the dominant approach to classical physics, the assumption of infinite precision, that quantities can be specified to an infinite number of digits, is taken for granted.

---

\*This is motivated by the observation that for two unit vectors  $\mathbf{n}_1$  and  $\mathbf{n}_2$  perpendicular to the unit vector pointing along  $(\theta_0, \phi_0)$ ,  $\Delta(\mathbf{S} \cdot \mathbf{n}_1)\Delta(\mathbf{S} \cdot \mathbf{n}_2) = 1/4$  for any state on the Bloch sphere.

A new paradigm that is emerging questions this assumption. In this approach, classical states can no longer be thought of as being represented by infinitely precise points in phase space. Instead, phase space densities become a more accurate description. Once such a description is admitted, many properties of systems that have traditionally been held to be exclusively quantum become natural in classical physics too.<sup>2,12-16</sup>

One such property is the non-separability of states. In the context of quantum mechanics, this is known as entanglement. In analogy with the definition of entanglement in the Wigner function formalism, we have motivated a classical analogue. We have then shown how this illumines the discussion on quantum chaos in particular, and the classical-quantum correspondence in general.

The system that we have chosen to demonstrate the utility of this concept on is the kicked top model. It is one of the most extensively studied systems in the context of quantum chaos. Not only has it been used as a testbed for many ideas in the field, but it has also led to novel insights. One of the most interesting features of this model is the relationship between entanglement and classical dynamics. Notably, a correlation has been observed between higher entanglement entropy and chaos.<sup>1,4-7</sup>

In this paper, we have first made the comparison concrete by computing a quantity on the classical side of the story, namely classical fluctuations of total angular momentum  $(\Delta J)^2/J^2$ , to predict the variation of entanglement entropy on the quantum side. Then, proceeding towards our main goal, we have calculated classical non-separability as quantified by mutual information as a function of the initial conditions, and compared it with entanglement entropy. A remarkable correlation is observed between the two quantities. The significance of this result is two-fold: (i) it opens up a new avenue of understanding in quantum chaos because the conceptual similarity of mutual information and entanglement enables a deeper and more transparent understanding of the chaos-entanglement connection; (ii) it demonstrates that this alternative paradigm of classical physics, far from being a mere philosophy, enables us to see connections that would have otherwise been hidden from view.

While this program has been successful for the kicked top, it remains to be seen whether its success can be extended to more general situations and other models as well, such as the Jaynes-Cummings and Dicke models where the chaos-entanglement connection has also been observed.<sup>8,9</sup> Moreover, we also need to compare entanglement growth with the growth of mutual information with time. A more careful analysis will be needed to see if the law of entanglement growth governed by Lyapunov exponents holds for mutual information too.<sup>7,10</sup> Another direction of interest could be to study more general situations of entangled systems, such as the quantum phases of matter where entanglement plays a key role, to see if classical analogues are possible there. We leave these questions as topics for future investigations.

## Acknowledgement

B.K. would like to acknowledge the contribution of Prof. Basit Bilal Koshul in shaping the conceptual outlook of this work. We would also like to thank Prof. Nicolas Gisin and Prof. Nima Lashkari for many useful suggestions and discussion.

**Funding:** We acknowledge funding from the Office of Science through the Quantum Science Center (QSC), a National Quantum Information Science Research Center, and the U.S. Department of Energy (DOE) (Office of Basic Energy Sciences), under Award No. DE-SC0019215.

## References

- (1) Neill, C.; Roushan, P.; Fang, M.; others Ergodic dynamics and thermalization in an isolated quantum system. *Nature Phys* **2016**, *12*, 1037–1041.
- (2) Del Santo, F.; Gisin, N. Physics without determinism: Alternative interpretations of classical physics. *Phys. Rev. A* **2019**, *100*, 062107.
- (3) Berry, M. V. The Bakerian Lecture, 1987. Quantum chaology. *Proc. R. Soc. Lond. A* **1987**, *413*, 183–198.
- (4) Chaudhry, S.; Smith, A.; Anderson, B.; others Quantum signatures of chaos in a kicked top. *Nature* **2009**, *461*, 768–771.
- (5) Wang, X.; Ghose, S.; Sanders, B. C.; Hu, B. Entanglement as a signature of quantum chaos. *Phys. Rev. E* **2004**, *70*, 016217.
- (6) Zou, Z.; Wang, J. Pseudoclassical Dynamics of the Kicked Top. *Entropy* **2022**, *24*.
- (7) Lerose, A.; Pappalardi, S. Bridging entanglement dynamics and chaos in semiclassical systems. *Phys. Rev. A* **2020**, *102*, 032404.
- (8) Furuya, K.; Nemes, M. C.; Pellegrino, G. Q. Quantum Dynamical Manifestation of Chaotic Behavior in the Process of Entanglement. *Phys. Rev. Lett.* **1998**, *80*, 5524–5527.
- (9) Hou, X.-W.; Hu, B. Decoherence, entanglement, and chaos in the Dicke model. *Phys. Rev. A* **2004**, *69*, 042110.
- (10) Zurek, W. H.; Paz, J. P. Quantum chaos: a decoherent definition. *Physica D: Nonlinear Phenomena* **1995**, *83*, 300–308, Quantum Complexity in Mesoscopic Systems.
- (11) Haake, F.; Kuś, M.; Scharf, R. Classical and quantum chaos for a kicked top. *Z. Physik B - Condensed Matter* **1987**, *65*, 381–395.

- (12) Gisin, N. In *Time in Physics*; Renner, R., Stupar, S., Eds.; Springer International Publishing: Cham, 2017; pp 1–15.
- (13) Lighthill, J.; Thompson, J. M. T.; Sen, A. K.; Last, A. G. M.; Tritton, D. T.; Mathias, P. The Recently Recognized Failure of Predictability in Newtonian Dynamics [and Discussion]. *Proceedings of the Royal Society of London. Series A, Mathematical and Physical Sciences* **1986**, *407*, 35–50.
- (14) Prigogine, I. *From Being to Becoming: Time and Complexity in the Physical Sciences*; W. H. Freeman and Company: New York, 1980; Chapter 2.
- (15) Ballentine, L. E. In *Fundamental Problems in Quantum Physics*; Ferrero, M., van der Merwe, A., Eds.; Springer Netherlands: Dordrecht, 1995; pp 15–28.
- (16) Arkhipov, A. Non-Separability of Physical Systems as a Foundation of Consciousness. *Entropy (Basel)* **2022**, *24*, 1539.
- (17) Peirce, C. S. In *The Collected Papers of Charles Sanders Peirce, Vol. I: The Principles of Philosophy*; Hartshorne, C., Weiss, P., Eds.; Harvard University Press: Cambridge, 1931; Chapter 3: Notes on Scientific Philosophy.
- (18) Styer, D. F.; Balkin, M. S.; Becker, K. M.; others Nine formulations of quantum mechanics. *American Journal of Physics* **2002**, *70*, 288–297.
- (19) Case, W. B. Wigner functions and Weyl transforms for pedestrians. *American Journal of Physics* **2008**, *76*, 937–946.
- (20) Myrvold, W. In *The Stanford Encyclopedia of Philosophy*, Fall 2022 ed.; Zalta, E. N., Ed.; Metaphysics Research Lab, Stanford University, 2022.

# Supporting Information Available

## S-I Classical Fluctuations with Time

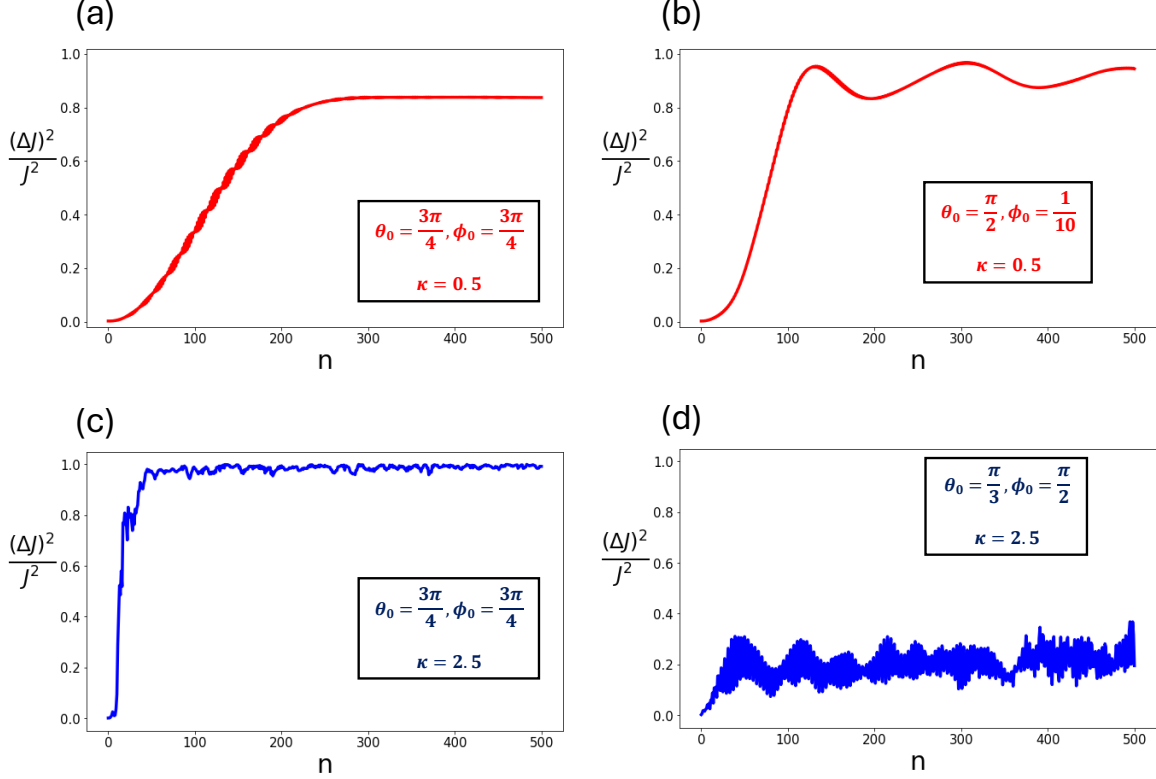


Figure 8: **Time evolution of classical fluctuations.** These plots were obtained by first using eqs. (4) to evolve 100 uniformly chosen initial points from a cloud centered at  $(\theta_0, \phi_0)$  with angular spread  $\sin \theta_0 \Delta \theta \Delta \phi = 1/J$  for  $J = 100$ . The values of  $(\Delta J)^2/J^2 = \langle \mathbf{X}^2 \rangle - \langle \mathbf{X} \rangle^2$  were then computed by averaging over the corresponding 100 trajectories.

In Fig. 8, some typical variations in  $(\Delta J)^2/J^2$  with time for  $\kappa = 0.5$  [(a) and (b)] and  $\kappa = 2.5$  [(c) and (d)] have been shown. For these plots, we took  $J = 100$  and averaged over 100 trajectories initialized at 100 uniformly chosen points.

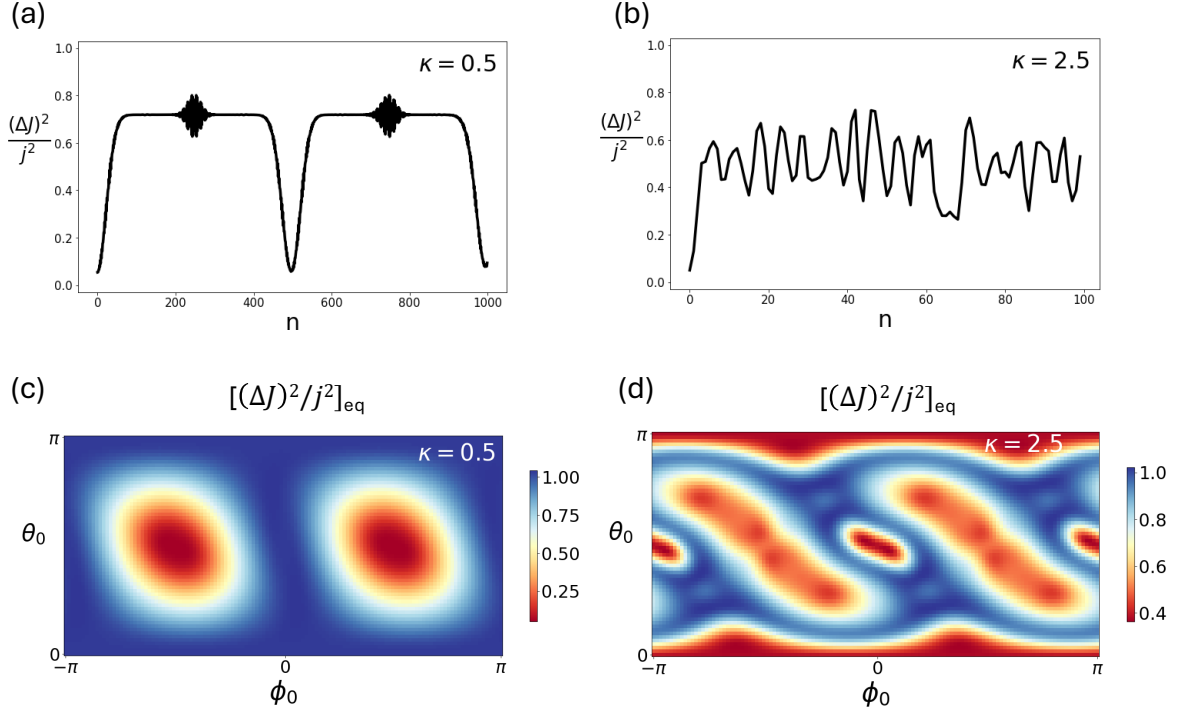


Figure 9: **Quantum fluctuations.** (a) and (b) show  $(\Delta J)^2/j^2$  as a function of the number of time steps  $n$  with the initial state  $(\theta_0 = 3\pi/4, \phi_0 = 3\pi/4)$  for  $\kappa = 0.5$  and  $\kappa = 2.5$  respectively. (c) and (d) show our estimates for the equilibrium values of  $(\Delta J)^2/j^2$  as a function of  $(\theta_0, \phi_0)$ . For (c)  $\kappa = 0.5$ , the estimate was obtained by averaging the values of  $(\Delta J)^2/j^2$  over  $60 \leq n \leq 100$ , whereas for (d)  $\kappa = 2.5$ , the average was performed over  $20 \leq n \leq 40$ .

## S-II Quantum Fluctuations

In fig. 9 we plot the quantum fluctuations  $(\Delta J)^2/j^2$  as a function of time and the initial orientation  $(\theta_0, \phi_0)$  for  $j = 20$  (or equivalently  $N = 40$ ). In fig. 9(a) and (b), we show the fluctuations as a function of the number of time steps starting with  $(\theta_0 = 3\pi/4, \phi_0 = 3\pi/4)$  for  $\kappa = 0.5$  and  $\kappa = 2.5$  respectively. Then in fig. 9(c) and (d), we estimate the equilibrium value of  $(\Delta J)^2/j^2$  as a function of the initial conditions  $(\theta_0, \phi_0)$  by averaging over multiple time steps for each  $\kappa$ . For  $\kappa = 0.5$ , the average is performed between  $60 \leq n \leq 100$ , whereas for  $\kappa = 2.5$ , the average is computed over  $20 \leq n \leq 40$ .

### S-III Update of Angular Momentum

To compute  $\mathbf{J}'_1 = U^\dagger \mathbf{J}_1 U$ , we first note that  $U_{z^2}^\dagger \mathbf{J}_1 U_{z^2}$  is as follows<sup>11</sup>

$$\begin{aligned}
U_{z^2}^\dagger J_{1x} U_{z^2} &= \frac{1}{2} (J_{1x} + iJ_{1y}) e^{i\frac{\kappa}{j}(J_{1z} + \frac{1}{2})} + \text{h.c.} \\
U_{z^2}^\dagger J_{1y} U_{z^2} &= \frac{1}{2i} (J_{1x} + iJ_{1y}) e^{i\frac{\kappa}{j}(J_{1z} + \frac{1}{2})} + \text{h.c.} \\
U_{z^2}^\dagger J_{1z} U_{z^2} &= J_{1z}.
\end{aligned} \tag{15}$$

On the other hand,  $U_{12}^\dagger \mathbf{J}_1 U_{12}$  simply rotates  $\mathbf{J}_1$  in the following way

$$\begin{aligned}
U_{12}^\dagger J_{1x} U_{12} &= J_{1x} \cos\left(\kappa \frac{J_{2z}}{j}\right) - J_{1y} \sin\left(\kappa \frac{J_{2z}}{j}\right) \\
U_{12}^\dagger J_{1y} U_{12} &= J_{1x} \sin\left(\kappa \frac{J_{2z}}{j}\right) + J_{1y} \cos\left(\kappa \frac{J_{2z}}{j}\right) \\
U_{12}^\dagger J_{1z} U_{12} &= J_{1z}.
\end{aligned} \tag{16}$$

Combining (15) and (16), we get

$$\begin{aligned}
U_{12}^\dagger U_{z^2}^\dagger J_{1x} U_{z^2} U_{12} &= \frac{1}{2} (J_{1x} + iJ_{1y}) e^{i\frac{\kappa}{j}(J_{1z} + J_{2z} + \frac{1}{2})} + \text{h.c.} \\
U_{12}^\dagger U_{z^2}^\dagger J_{1y} U_{z^2} U_{12} &= \frac{1}{2i} (J_{1x} + iJ_{1y}) e^{i\frac{\kappa}{j}(J_{1z} + J_{2z} + \frac{1}{2})} + \text{h.c.} \\
U_{12}^\dagger U_{z^2}^\dagger J_{1z} U_{z^2} U_{12} &= J_{1z}.
\end{aligned} \tag{17}$$

Finally, performing the rotation around the y-axis gives us the following answer for  $\mathbf{J}'_1 =$

$$U^\dagger \mathbf{J}_1 U = U_y^\dagger U_{12}^\dagger U_{z^2}^\dagger \mathbf{J}_1 U_{z^2} U_{12} U_y,$$

$$\begin{aligned}
J'_{1x} &= \frac{1}{2} (J_{1z} + iJ_{1y}) e^{-i\frac{\kappa}{j}(J_{1x} + J_{2x} + \frac{1}{2})} + \text{h.c.} \\
J'_{1y} &= \frac{1}{2i} (J_{1z} + iJ_{1y}) e^{-i\frac{\kappa}{j}(J_{1x} + J_{2x} + \frac{1}{2})} + \text{h.c.} \\
J'_{1z} &= -J_{1x}.
\end{aligned} \tag{18}$$